Title
ON THE BEHAVIOR OF SMALL FATIGUE CRACKS IN COMMERCIAL ALUMINUM-LITHIUM ALLOYS

Authors
Rao, K.T.V.
Yu, W.
Ritchie, R.O.

Publication Date
1987-06-01

Center for Advanced Materials

CAM REPORT

Submitted to Engineering Fracture Mechanics

On the Behavior of Small Fatigue Cracks in Commercial Aluminum-Lithium Alloys

K.T. Venkateswara Rao, W. Yu, and
R.O. Ritchie

June 1987

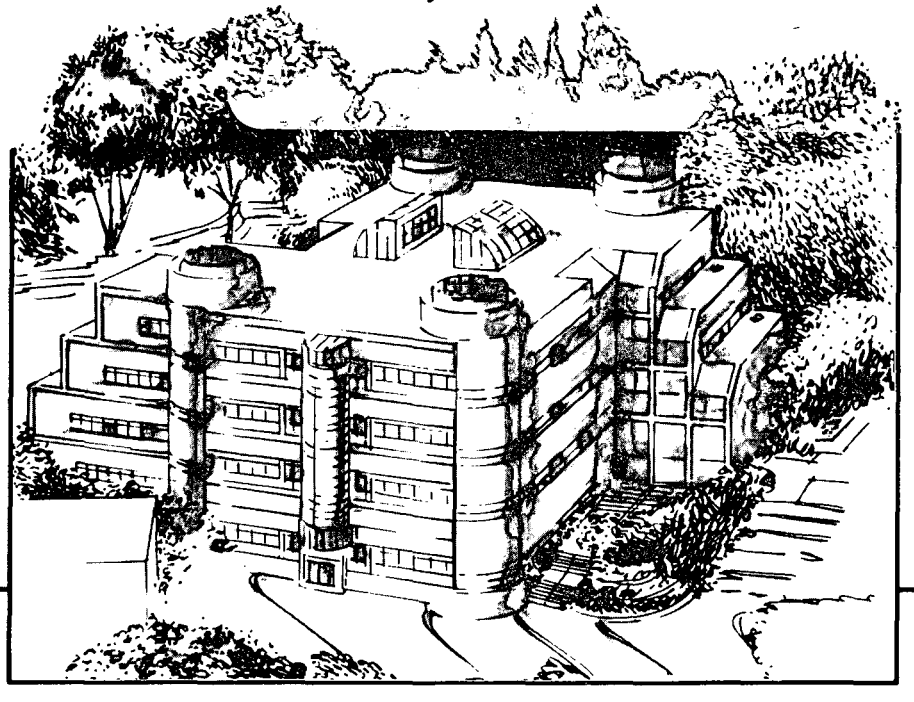

Materials and Chemical Sciences Division

Lawrence Berkeley Laboratory • University of California

ONE CYCLOTRON ROAD, BERKELEY, CA 94720 • (415) 486-4755

Prepared for the U.S. Department of Energy under Contract DE-AC03-76SF00098

DISCLAIMER

LBL-23680

ON THE BEHAVIOR OF SMALL FATIGUE CRACKS IN COMMERCIAL ALUMINUM-LITHIUM ALLOYS

K. T. Venkateswara Rao, W. Yu and R. O. Ritchie

Center for Advanced Materials, Lawrence Berkeley Laboratory, and
Department of Materials Science and Mineral Engineering
University of California, Berkeley, CA 94720

June 1987

submitted to Engineering Fracture Mechanics

This work was supported by the Director, Office of Energy Research, Office of Basic Energy Sciences, Materials Sciences Division of the U.S. Department of Energy under Contract No. DE-AC03-76SF00098.

ON THE BEHAVIOR OF SMALL FATIGUE CRACKS IN COMMERCIAL ALUMINUM-LITHIUM ALLOYS

K. T. Venkateswara Rao, W. Yu and R. O. Ritchie

Center for Advanced Materials, Lawrence Berkeley Laboratory, and
Department of Materials Science and Mineral Engineering
University of California, Berkeley, CA 94720, U.S.A.

Abstract--The fatigue crack propagation behavior of naturally-occurring, microstructurally-small (1-1000 μm), surface cracks is examined as a function of microstructure in commercial aluminum-lithium alloys 2090-T8E41, 8091-T351 and 2091-T351, and results compared with behavior in traditional high-strength aluminum alloys 2124 and 7150. Despite large differences in the fatigue crack propagation behavior of long (≥10 μm) cracks in these alloys, little difference is observed in the small crack growth resistance, with the small crack growth rates for all microstructures lying within a scatterband some 2-4 orders of magnitude higher than the near-threshold fatigue behavior of long cracks. Such results are attributed primarily to a lack of crack tip shielding (developed from crack deflection and resulting crack closure from asperity wedging) with small cracks of limited wake. Since the well-known superior fatigue crack growth resistance of aluminum-lithium alloys can be traced principally to such shielding, promoted by the branched and tortuous nature of their crack paths, the "anomaly" between long and small crack behavior appears to be most significant in these alloys.

INTRODUCTION

Durability and damage-tolerance in safety-critical components and structures is of prime importance for modern aerospace applications. Such factors are generally assessed using fracture mechanics-based methodologies, where for example it is assumed that flaws pre-exist from the initial loading cycle, and the lifetime of the structure is estimated as the number of cycles to propagate such a flaw to failure. Such damage-tolerant life prediction procedures, as for example specified in the U.S. Air Force mandatory

specification MIL-A-83444, require a knowledge of the rate of growth of fatigue cracks in the particular microstructure under representative environmental and loading conditions (1). This is generally specified as experimental data plots showing growth rates (da/dN) as a function of the stress intensity range (ΔK), which are then integrated from initial to final crack sizes to determine life.

Although considered inherently to be conservative as the crack initiation life is assumed to be zero, a potential problem with this approach can arise from the "anomalous" behavior of cracks which are physically small ($\lesssim 1$ mm) or which approach the dimensions of microstructure or local plasticity (2). Such small cracks are now known to propagate at stress intensities well below the fatigue threshold, ΔK_{TH}, below which fatigue cracks are presumed dormant, and in general to grow at rates far in excess of long ($\gtrsim 10$ mm) cracks at the same (nominal) stress intensity range (2-7). Since damage-tolerant life analyses are biased by low growth rate data and invariably utilize long crack results, there is thus strong potential for non-conservative life prediction.

The newly developed advanced aluminum-lithium alloys are of particular interest in this regard, as despite their unquestionably superior (long) fatigue crack growth properties compared to traditional high strength aluminum alloys (8-14), the discrepancy between long and small crack propagation behavior in these alloys has recently been shown to be extremely large (15,16). In view of the importance of the "small crack" effect in potential airframe and fuel tank materials, the objective of this study was thus to document the

growth rate characteristics of small (1-1000 μm), naturally-occurring surface cracks in a series of commercial aluminum-lithium alloys, and to compare such behavior with that measured (17) in traditional high strength 2124 and 7150 aluminum alloys. It is shown that despite small crack growth rates which are some 2 to 4 orders of magnitude faster than long crack behavior, the small crack fatigue properties of aluminum-lithium alloys remain comparable to that of 2124 and 7150 alloys.

EXPERIMENTAL PROCEDURES

Materials

Commercial 25 mm thick plates of 2124 and 7150 and 11 - 15 mm thick plates of 2090, 2091 and 8091 were obtained with nominal composition shown in Table I. All alloys were tested in their recommended commercial temper condition, although the 2124 and 7150 alloys were additionally examined at several other tempers. Details of the aging treatments are given in Table II. Room temperature mechanical properties for the longitudinal orientation (L-T orientation for K_{Ic} values) are listed in Table III.

Microstructures

All alloys show tend to show a pancake-shaped grain structure elongated along the rolling direction, with a greater degree of anisotropy and general lack of recrystallization in the lithium-containing alloys. Respective grain sizes are shown in Table IV, together with the primary hardening precipitates. Microstructures in

Table I. Various commercial aluminum alloys investigated and their nominal chemical compositions in wt.%.

		Li	Cu	Mg	Zn	Fe	Si	Ti	Zr	Al
ALCOA	2124	--	4.50	1.50	0.25	0.30	0.20	0.15	--	bal
ALCOA	7150	--	2.10	2.16	6.16	0.11	0.07	0.02	0.13	bal
ALCOA	2090	2.05	2.86	0.01	0.005	0.02	0.01	0.02	0.12	bal
PECHINEY	2091	1.7-2.3	1.8-2.5	1.1-1.9	0.25	0.3	0.2	0.1	0.04-0.16	bal
ALCAN	8091	2.60	1.90	0.90	--	0.20	0.10	--	0.12	bal

Table II. Heat treatments utilized on aluminum alloys to obtain the different microstructures.

Alloy	Condition		Heat Treatment
2124	T351	(underaged)	solution treat, 2% stretch, naturally aged
	T751	(overaged)	solution treat, 2% stretch, 48 hr at 190°C
7150	T351	(underaged)	solution treat, 2% stretch, 1.5 hr at 121°C
	T651	(peak aged)	solution treat, 2% stretch, 100 hr at 121°C
	T751	(overaged)	solution treat, 2% stretch, 24 hr at 121°C + 40 hr at 163°C
2090	T8E41	(peak aged)	solution treat, 6% stretch, 24 hr at 163°C
2091	T351	(underaged)	solution treat, 1-3% stretch, naturally aged
8091	T351	(underaged)	solution treat, 1-3% stretch, naturally aged

Table III. Room temperature mechanical properties of the various commercial aluminum alloys investigated.

Alloy	Yield Strength (MPa)	U.T.S. (MPa)	% Elongation (on 25 mm)	Fracture Toughness K_{Ic} (MPa$\sqrt{m}$)
2124-T351	360	488	17.8	24
2124-T751	370	440	10.2	42
7150-T351	371	485	6.8	37
7150-T651	404	480	6.0	21
7150-T751	372	478	7.1	29
2090-T8E41	552	589	9.3	35
2091-T351	517	633	10.3	28
8091-T351	309	417	10.7	39

2124 are recrystallized and show evidence of GP zones and several constituent phases, including Al_7Cu_2Fe, $Al_{12}(Fe,Mn)_3Si$, Mg_2Si and Al_2CuMg (17). In 7150, 4 to 8 nm diameter GP zones are present in underaged structures, which are replaced by semi-coherent η' precipitates ($MgZn_2$-$Mg(CuAl)_2$) on peak aging, and coarsened matrix η' and incoherent η precipitates ($MgZn_2$ compounds) in both matrix and grain boundaries on overaging (18). The aluminum-lithium alloys, on the other hand, are primarily unrecrystallized and hardened by a combination of coherent, matrix precipitates. In the peak aged Al-Cu-Li alloy 2090, these include spherical δ' (Al_3Li), plate-like T_1 (Al_2CuLi) and θ' (Al_2Cu), with β' (Al_3Zr) dispersoids.* The underaged Al-Cu-Li-Mg alloy 2091, conversely, shows a small degree of

*Earlier studies (e.g., ref. 19) refer to the T_1 and θ' precipitates as T_1' and T_2', respectively. Here, T_1 and θ' refer to plate-like precipitates with the (111) and (100) habits, respectively.

Table IV. Microstructure and grain sizes of alloys tested

Alloy	Grain Size L (mm)	L-T (μm)	S-T (μm)	Primary Hardening Precipitates
2124-T351 2124-T751	0.7	350	50	GP zones Θ ($CuAl_2$), Al_7Cu_2Fe, $Al_{12}(Fe,Mn)_3Si$, Mg_2Si
7150-T351 7150-T651 7150-T751	2-3	750	30	GP zones η' ($MgZn_2$-$Mg(CuAl)_2$) matrix η', η ($MgZn_2$ compounds)
2090-T8E41	2-3	500	50	δ' (Al_3Li), T_1 (Al_2CuLi), Θ' (Al_2Cu)
2091-T351	1-2	600	40	δ', S (Al_2CuMg)
8091-T351	0.25	65	25	δ', S

recrystallization, a lower volume fraction of δ' and evidence of fine, needle-like S precipitates (precursor to Al_2CuMg). Similarly, the major strengthening precipitates in the underaged Al-Li-Cu-Mg alloy 8091 are δ' and S precipitates (20,21).

Fatigue testing

To examine the early growth of naturally-occurring, microstructurally-small (1-1000 μm) surface cracks, fatigue tests were performed by acetate replication techniques on smooth, unnotched, rectangular specimens cycled in four-point bending (Fig. 1a) in room temperature air (22°C, 45% relative humidity) using electro-servo-hydraulic testing machines. Tests were conducted at a cyclic frequency of 50 Hz (sine wave) with a load ratio ($R = P_{min}/P_{max}$) of 0.1, where the maximum bending stresses on the top

surface did not exceed 0.9 times the yield stress. Due to the high strength and poor short-transverse properties of 2090-T8E41, tests in this alloy were carried out on waisted specimens (Fig. 1b) to minimize the occurrence of mid-section delamination cracks in the plane of loading, where the shear stresses are a maximum.

Tests were interrupted approximately every 5,000 to 10,000 cycles and held at the mean load to permit replication of the electropolished and lightly etched specimen surface. Growth rates ($\Delta a/\Delta N$) were then computed in terms of the mean crack extension within such time increments. Typical initiation lives (i.e., to detect a 0.5 mm visible crack) varied between 1-4 x 10^5 cycles. Cellulose acetate replicas were subsequently gold coated using sputtering techniques to gain improved crack length resolution.

As computed plastic zone sizes remained small (typically 4%) compared to crack size, characterization of small-crack growth rates in terms of the nominal stress intensity range ($\Delta K = K_{max} - K_{min}$) was deemed to be appropriate. Stress intensity factors were computed using the Newman and Raju equation (22) for semi-elliptical surface flaws assuming an a/c (crack depth to half the surface crack length) ratio of 0.8, based on serial sectioning experiments. Owing to the high degree of crack deflection and meandering, crack lengths were measured as the projected lengths normal to the bending tensile stresses using optical microscopy. With such procedures, detection of crack increments of 1 to 5 μm was possible such that crack growth rates as low as 5 x 10^{-10} m/cycle could be readily monitored.

For comparison, conventional crack growth tests on long

($\gtrsim$10 mm) cracks were performed under identical loading and environmental conditions, on 6.35 mm thick compact C(T) specimens. Crack length and crack closure were continuously monitored using D.C. electrical potential and back-face strain compliance (17) techniques, respectively. Growth rates were characterized both in terms of the nominal stress intensity range ΔK and the effective stress intensity range ΔK_{eff}, defined as $K_{max} - K_{cl}$, where K_{cl} is the closure stress intensity where the unloading compliance curve first deviates from linearity. Fracture surfaces and crack path morphologies were examined with scanning electron microscopy.

RESULTS

Long crack behavior

Long fatigue crack growth behavior in the eight alloys is plotted as a function of ΔK in Fig. 2. It is readily apparent that the aluminum-lithium alloys 2090, 8091 and 8090 in general show the lowest growth rates in comparison to the traditional 2124 and 7150 alloys, although at near-threshold levels growth rates in the underaged microstructures of 2124 and 7150 become comparable. The superior long crack performance of the aluminum-lithium alloys is particularly evident at higher stress intensity ranges, typically above 4 MPa$\sqrt{m}$, where for example growth rates are between 5 and 50 times slower than than in peak aged or overaged 7150. Of the aluminum-lithium alloys, optimum crack growth resistance is seen in the higher strength 2090-T8E41 alloy. The excellent long crack fatigue properties of these alloys have been attributed primarily to

crystallographic crack growth and enhanced crack meandering (10-14), induced by the marked slip planarity and deformation texture (particularly in 2090) which is characteristic of the commercial alloys. The occurrence of such tortuous crack paths in turn promotes significant crack tip shielding (17), i.e., a reduction in the **local** stress intensity experienced at the crack tip, through mechanisms of crack deflection (23) and resulting (roughness-induced) crack closure from the wedging of fracture surface asperities (24-26), which leads to reduced growth rates.

Small crack behavior in 2124 and 7150

The behavior of small cracks in underaged and overaged microstructures of 2124 and underaged, peak aged and overaged microstructures of 7150 are shown in Fig. 3. Data are plotted as a function of ΔK and are compared with long crack results from Fig. 2. There is clearly significant scatter in the small crack results, although this is to be expected as growth rates are measured at microstructural dimensions and thus reflect the local variations in crack velocity as the crack encounters various features in the microstructure. Despite this scatter, it is clear that the growth rates of the small cracks invariably exceed those of long cracks at equivalent ΔK levels, similar to behavior reported in other alloys (e.g., refs. 2-7,15-17). The effect becomes most pronounced with decreasing growth rates, such that at near-threshold levels, the propagation rates of small cracks can be 2 to 3 orders of magnitude faster than long cracks. More importantly, the small flaws appear to

propagate at stress intensities well **below** ΔK_{TH}, with no apparent sign of an intrinsic threshold.

Of further interest is that, unlike long crack behavior, the small crack results in both 2124 and 7150 appear to be far less sensitive to microstructure. For example, the distinctly superior crack growth properties of the underaged microstructures, which are so apparent for long cracks, are simply not evident in the small crack results (Fig. 3). However microstructurally, the small cracks do tend to show a decreasing tendency for crack deflection with increased aging, similar to observations for long cracks.

Small crack behavior in aluminum-lithium alloys

Corresponding growth rate properties of small cracks in the aluminum-lithium alloys are shown in Fig. 4. Results for various orientations in 2090-T8E41 (Fig. 4a) and in the T351 temper of both 2091 and 8091 (Fig. 4b) are plotted as a function of ΔK and are compared with long crack data. Behavior appears essentially to be similar to 2124 and 7150 in that small cracks grow at rates far faster than long cracks at equivalent near-threshold levels, and further continue to propagate at stress intensity ranges as low as 0.7 $MPa\sqrt{m}$, well below the long crack threshold ΔK_{TH}. However, in view of the generally superior long crack properties of aluminum-lithium alloys (Fig. 2), the discrepancy between long and small crack growth rates in these alloys is larger, with small cracks propagating up to 4 orders of magnitude faster than long cracks at equivalent near-threshold levels.

Microstructurally, the early growth of such small flaws is illustrated in Fig. 5, based on scanning electron microscopy of gold coated acetate replicas in 2091-T351. Cracks initiate from particles and grow initially in linear fashion. However, with increasing crack length, they begin to show evidence of deflection and branching, and presumably start developing crack closure, which with sufficient crack size ultimately approaches that of a long crack.

DISCUSSION

It is now generally accepted that the fatigue behavior of long cracks is strongly influenced by crack closure (and crack deflection) mechanisms, particularly at lower growth rates below typically 10^{-8} m/cycle (27). Crack closure and deflection represent a general class of "toughening" mechanisms known as crack tip shielding, which act to reduce the **local** "driving force" actually experienced at the crack tip (17). In high strength aluminum alloys, where the prominent mechanisms of shielding result from the wedging of fracture surface asperities (and to a lesser extent corrosion debris) and from crack deflection, superior fatigue crack growth properties are generally observed in coherent-particle hardened microstructures, as the resulting planar slip promotes deflected and meandering crack paths and consequently rough fracture surfaces. It is primarily for this reason that (long) crack growth rates tend to be slower in underaged microstructures in traditional alloys such as 2124 and 7150. Moreover, this notion is particularly relevant to aluminum-lithium alloys, where crack paths are especially tortuous due to the marked

planarity of slip from the δ' precipitation and, in the 2090 alloy (13,14), from the strong anisotropy/texture which is imparted by commercial thermomechanical heat treatments and lack of recrystallization. As the deflected crack path morphology persists to ΔK levels as high as $\sim$20 MPa$\sqrt{m}$ in these materials (13), aluminum-lithium alloys tend to show generally superior (long) crack growth properties over a wide spectrum of growth rates.

The major contribution of crack tip shielding to fatigue crack growth resistance in aluminum alloys and particularly aluminum-lithium alloys has important implications to their fatigue properties in general. First, as the prominent source of shielding results from wedges inside the crack, the effect of such roughness-induced closure will be minimized at high mean stresses where the mean crack opening displacements are larger, resulting in large load ratio effects, particularly at near-threshold levels(14). Moreover, in the presence of continuous or periodic compression cycles, growth rates may similarly be increased as the compressive loads can reduce the magnitude of closure through the crushing of fracture surface asperities (28). Accordingly, when compression overloads are applied to arrested cracks at ΔK_{TH}, significant crack growth can result at stress intensities at, or even below, the threshold (13,28).

More importantly, shielding mechanisms act primarily on the wake of the crack, and thus are sensitive to crack size (17). The implication of this is that due to their limited wake, microstructurally-small cracks are unlikely to be as affected by shielding as long cracks, and thus, at the same nominal ΔK,

experience a larger effective near-tip "driving force". In fact, in situ closure stress measurements on small cracks have indicated negligible closure levels in 2090 and similar alloys (16). It is considered that this is the primary reason for the accelerated and "sub-threshold" growth rates of small cracks, as illustrated for the eight aluminum alloys in Figs. 3 and 4. However, with increasing length such cracks begin to develop closure (16,17) such that growth rates merge with long crack data once shielding levels approach that of long flaws. In the present study, this apparently occurs at nominal ΔK levels of between 4 and 8 MPa$\sqrt{m}$, when crack lengths exceed approximately 700 to 1000 μm.

Explanations for the accelerated growth rates of small cracks based on closure arguments can be substantiated by comparing the small crack data with that of long cracks where the role of crack closure has been minimized. This is illustrated for 2090-T8E41 in Fig. 6, where it can be seen that the long and small crack growth rates come into closer correspondence when the long crack data are presented in terms of ΔK_{eff} instead of ΔK, i.e., where experimental measurements of K_{cl} are used to subtract out the closure contribution. Similarly, but a lesser extent, small crack growth rates correspond to long crack data measured at high load ratios ($R = 0.75$).* This implies that the behavior of small flaws largely reflects that of long cracks with minimal shielding.

---

*Recent studies by Hertzberg and co-workers (29) have shown that by measuring long crack growth rates under constant K_{max}/increasing K_{min} loading conditions, which minimize crack closure, a conservative estimate of $\Delta a/\Delta N$ vs. ΔK behavior for small cracks can be obtained, except at very low, sub-threshold stress intensities.

It is apparent from Fig. 6, however, that small flaws still propagate below the effective threshold, indicating that the small crack effect cannot be solely attributed to the closure concept, although this clearly is a prominent mechanism. Additional factors which have been identified as contributing to discrepancies in long and small crack behavior include enhanced crack tip opening strains (30), surface microplasticity (31), differences in crack geometry (32,33), interactions of small flaws with microstructural features of comparable dimensions (31,34,35), and definition of an appropriate "crack driving force" (36). Moreover, since naturally occurring, small cracks initiate at "weak links" in the microstructure, forming crack fronts which encompass only relatively few grains, unlike through-thickness long cracks their growth will not be averaged over many disadvantageously oriented grains (7).

Finally, as long cracks in lithium-containing aluminum alloys tend to develop the most shielding due to their extremely tortuous crack paths, the difference between long and small crack growth rates appears to be maximized in these materials. However, when compared with behavior in other aluminum alloys, small crack growth rates in 2090-T8E41, 2091-T351 and 8091-T351 are actually no worse than results for 2124 and 7150, as shown in Fig. 7. Moreover, strength levels in the 2090 and 2091 alloys are some 35 to 50% higher than in 2124 and 7150. Although there is considerable inherent scatter in the small crack data, it is apparent that, in contrast to long crack behavior (Fig. 2), small crack growth rates in aluminum alloys are comparatively less sensitive to both microstructure and composition

(including aging condition and strength level). Since long crack data at higher growth rates and at high load ratios are similarly less sensitive to microstructure (e.g., ref. 17), this suggests that the origin of microstructural effects on fatigue crack propagation behavior in aluminum alloys results primarily from shielding mechanisms. Moreover, since slip planarity and grain size (and hence morphology of crack path) are known to be relevant, it would appear that crack deflection and resulting roughness-induced crack closure provide the major contribution.

CONCLUSIONS

Based on a comparison of the fatigue behavior of naturally-occurring, microstructurally-small (1-1000 μm) surface cracks in commercial aluminum-lithium 2090-T8E41, 2091-T351 and 8091-T351 alloys and traditional high strength 2124 and 7150 aluminum alloys, the following conclusions may be made:

1. Small fatigue crack growth rates in commercial aluminum alloys are up to 2-4 orders of magnitude faster than corresponding growth rates for long cracks at equivalent (nominal) stress intensity ranges. In contrast to long crack results, over a wide spectrum of growth rates from 10^{-10} to 10^{-6} m/cycle, the influence of microstructure and composition on small crack behavior is relatively minor.

2. The accelerated growth rate behavior of small cracks, which predominates below typically 10^{-8} m/cycle, is attributed primarily to a limited role of crack tip shielding with cracks of limited wake. In precipitation-hardened aluminum alloys, such shielding, which plays a

dominant role in the near-threshold fatigue behavior of long cracks, appears to result principally from crack deflection and consequent crack closure from the wedging of fracture surface asperities.

3. The discrepancy between long and small fatigue crack behavior appears to be maximized in aluminum-lithium alloys. This is in part due to their superior long crack properties which result from very high levels of shielding induced by severely deflected crack paths (promoted by a marked planarity of slip and strong deformation texture). However, although up to 4 orders of magnitude faster than long cracks, small crack growth rates in 2090, 2191 and 8091 remain comparable with behavior in traditional alloys, such as 2124-T351 and 7150-T751.

Acknowledgements--The work was supported by the Director, Office of Basic Energy Sciences, Materials Sciences Division of the U.S. Department of Energy under Contract No. DE-AC03-76SF00098, under the auspices of the Center for Advanced Materials, Lawrence Berkeley Laboratory. Results on 2124 and 7150 were funded by the U.S. Air Force Office of Scientific Research under Grant No. AFOSR 82-0181, with Dr. A. H. Rosenstein as contract monitor. Alloys were supplied by ALCOA, Northrop and AFWAL (the latter through the NAVAIR Collaborative Test Program). Thanks are due to Drs. Bretz, Bucci, Chanani, Petrak, Quist, Sawtell and Scarich for their advice and help in procuring materials, and to L. Rumaner and H. Hayashigatani for experimental assistance.

REFERENCES

1. Anon, Airplane damage tolerance requirements. Military Specification MIL-A-83444, U.S. Air Force (1974).

2. S. Suresh and R. O. Ritchie, The propagation of short fatigue cracks. Intl. Metals Rev., **29**, 445-476 (1984).

3. S. J. Hudak, Small crack behavior and the prediction of fatigue life. J. Engng. Mater. Technol., **103**, 26-35 (1981).

4. K. J. Miller, The short crack problem. Fatigue Engng. Mater. Struct., 5, 223-232 (1982).

5. J. Schijve, Differences between the growth of small and large fatigue cracks in relation to threshold K values, in Fatigue Thresholds (Edited by J. Bäcklund, A. F. Blom and C. J. Beevers), Vol. 2, pp. 881-908. EMAS Ltd., Warley, England (1982).

6. J. Lankford, Influence of microstructure in the growth of small fatigue cracks. Fatigue Fract. Engng. Mater. Struct., 8, 161-175 (1985).

7. R. O. Ritchie and J. Lankford, Small fatigue cracks: a statement of the problem and potential solutions. Mater. Sci. Engng., **84**, 11-16 (1986).

8. E. J. Coyne, T. H. Sanders, and E. A. Starke, The effect of microstructure and moisture on low cycle fatigue and fatigue crack propagation of two Al-Li-X alloys, in Aluminum-Lithium Alloys (Edited by T. H. Saunders and E. A. Starke), pp. 293-305. TMS-AIME, Warrendale, PA (1981).

9. F. S. Lin and E. A. Starke, The effect of Cu content and degree of recrystallization on the fatigue resistance of 7XXX-type aluminum alloys. II. Fatigue crack propagation. Mater. Sci. Engng., **43**, 65-76 (1980).

10. A. K. Vasudévan, P. E. Bretz, A. C. Miller, and S. Suresh, Fatigue crack growth behavior of aluminum alloy 2020 (Al-Cu-Li-Md-Cd). Mater. Sci. Engng., **64**, 113-122 (1984).

11. K. V. Jata and E. A. Starke, Fatigue crack growth and fracture toughness behavior of Al-Li-Cu alloy, in Metall. Trans. A, **17A**, 1011-1026 (1986).

12. J. Petit, S. Suresh, A. K. Vasudévan, and R. C. Malcolm, Constant amplitude and post-overload fatigue crack growth in Al-Li alloys, in Aluminium-Lithium Alloys III (Edited by C. Baker, P. J. Gregson, S. J. Harris, and C. J. Peel), pp. 257-262. Institute of Metals, London, England (1986).

13. W. Yu and R. O. Ritchie, Fatigue crack propagation in 2090 aluminum-lithium alloy: effect of compression overload cycles. J. Engng. Mater. Technol., **109**, 81-85 (1987).

14. K. T. Venkateswara Rao, W. Yu, and R. O. Ritchie, Fatigue crack propagation in aluminum-lithium alloy 2090: Part I. Long crack behavior. Metall. Trans. A, **18A** (1987), in press.

15. K. T. Venkateswara Rao, W. Yu, and R. O. Ritchie, On the growth of small fatigue cracks in aluminum-lithium alloy 2090. Scripta Met., 20, 1459-1464 (1986).

16. M. R. James, Growth behavior of small fatigue cracks in Al-Li-Cu alloys. Scripta Met., 21, 783-788 (1987).

17. R. O. Ritchie and W. Yu, Short crack effects in fatigue: a consequence of crack tip shielding, in Small Fatigue Cracks (Edited by R. O. Ritchie and J. Lankford), pp. 167-189. TMS-AIME, Warrendale, PA (1986).

18. E. Zaiken and R. O. Ritchie, Effects of microstructure on fatigue crack propagation and crack closure behavior in aluminum alloy 7150. Mater. Sci. Engng., 70, 151-160 (1985).

19. R. J. Rioja and E. A. Ludwiczak, Identification of metastable phases in Al-Cu-Li alloy (2090), in Aluminium-Lithium Alloys III (Edited by C. Baker, P. J. Gregson, S. J. Harris, and C. J. Peel), pp. 471-482. Institute of Metals, London, England (1986).

20. P. Meyer and B. Dubost, Production of aluminium-lithium alloy with high specific properties, in Aluminium-Lithium Alloys III (Edited by C. Baker, P. J. Gregson, S. J. Harris, and C. J. Peel), pp. 37-46. Institute of Metals, London, England (1986).

21. H. M. Flower and P. J. Gregson, Solid state phase transformations in aluminium alloys containing lithium. Mat. Sci. Tech., 3, 81-90 (1987).

22. J. C. Newman and I. S. Raju, An empirical stress-intensity factor equation for the surface crack. Engng. Fract. Mech., 15, 185-192 (1981).

23. S. Suresh, Crack deflection: implications for the growth of long and short fatigue cracks. Metall. Trans. A, 14A, 2375-2385 (1983).

24. N. Walker and C. J. Beevers, A fatigue crack closure mechanism in titanium. Fatigue Engng. Mater. Struct., 1, 135-148 (1979).

25. K. Minakawa and A. J. McEvily, On crack closure in the near-threshold region. Scripta Met., 15, 633-636 (1981).

26. S. Suresh and R. O. Ritchie, A geometric model for fatigue crack closure induced by fracture surface roughness. Metall. Trans. A, 13A, 1627-1631 (1982).

27. R. O. Ritchie, Thresholds for fatigue crack propagation: questions and anomalies, in Advances in Fracture Research '87, Proc. Sixth Intl. Conf. on Fracture (ICF-6) (Edited by S. R. Valluri), Vol. 1, pp. 235-260. Pergamon Press, Oxford, England (1984).

28. E. Zaiken and R. O. Ritchie, On the role of compression overloads in influencing crack closure and the threshold condition for fatigue crack growth in 7150 aluminum alloy. Engng. Fract. Mech., 22, 35-48 (1985).

29. R. W. Hertzberg, W. A. Herman, and R. O. Ritchie, Use of a constant K_{max} test procedure to predict small crack growth behavior in 2090-T8E41 aluminum-lithium alloy. Scripta Met., 21 (1987) in review.

30. J. Lankford and D. L. Davidson, The role of metallurgical factors in controlling the growth of small fatigue cracks, in Small Fatigue Cracks (Edited by R. O. Ritchie and J. Lankford), pp. 51-71. TMS-AIME, Warrendale, PA (1986).

31. M. R. James and W. L. Morris, The effect of microplastic surface deformation on the growth of small cracks, in Small Fatigue Cracks (Edited by R. O. Ritchie and J. Lankford), pp. 145-156, TMS-AIME, Warrendale, PA (1986).

32. L. Wagner, J. K. Gregory, A. Gysler, and G. Lütjering, Propagation behavior of short cracks in a Ti-8.6Al alloy, in Small Fatigue Cracks (Edited by R. O. Ritchie and J. Lankford), pp. 117-128. TMS-AIME, Warrendale, PA (1986).

33. A. Pineau, Short fatigue crack behavior in relation to three-dimensional aspects and crack closure effect, in Small Fatigue Cracks (Edited by R. O. Ritchie and J. Lankford), pp. 191-211. TMS-AIME, Warrendale, PA (1986).

34. K. Tanaka, Modeling of propagation and non-propagation of small fatigue cracks, in Small Fatigue Cracks (Edited by R. O. Ritchie and J. Lankford), pp. 343-361. TMS-AIME, Warrendale, PA (1986).

35. C. W. Brown and J. E. King, The relevance of microstructural influences in the short crack regime to overall fatigue resistance, in Small Fatigue Cracks (Edited by R. O. Ritchie and J. Lankford), pp. 73-95. TMS-AIME, Warrendale, PA (1986).

36. S. J. Hudak and K. S. Chan, In search of a driving force to characterize the kinetics of small crack growth, in Small Fatigue Cracks (Edited by R. O. Ritchie and J. Lankford), pp. 379-405. TMS-AIME, Warrendale, PA (1986).

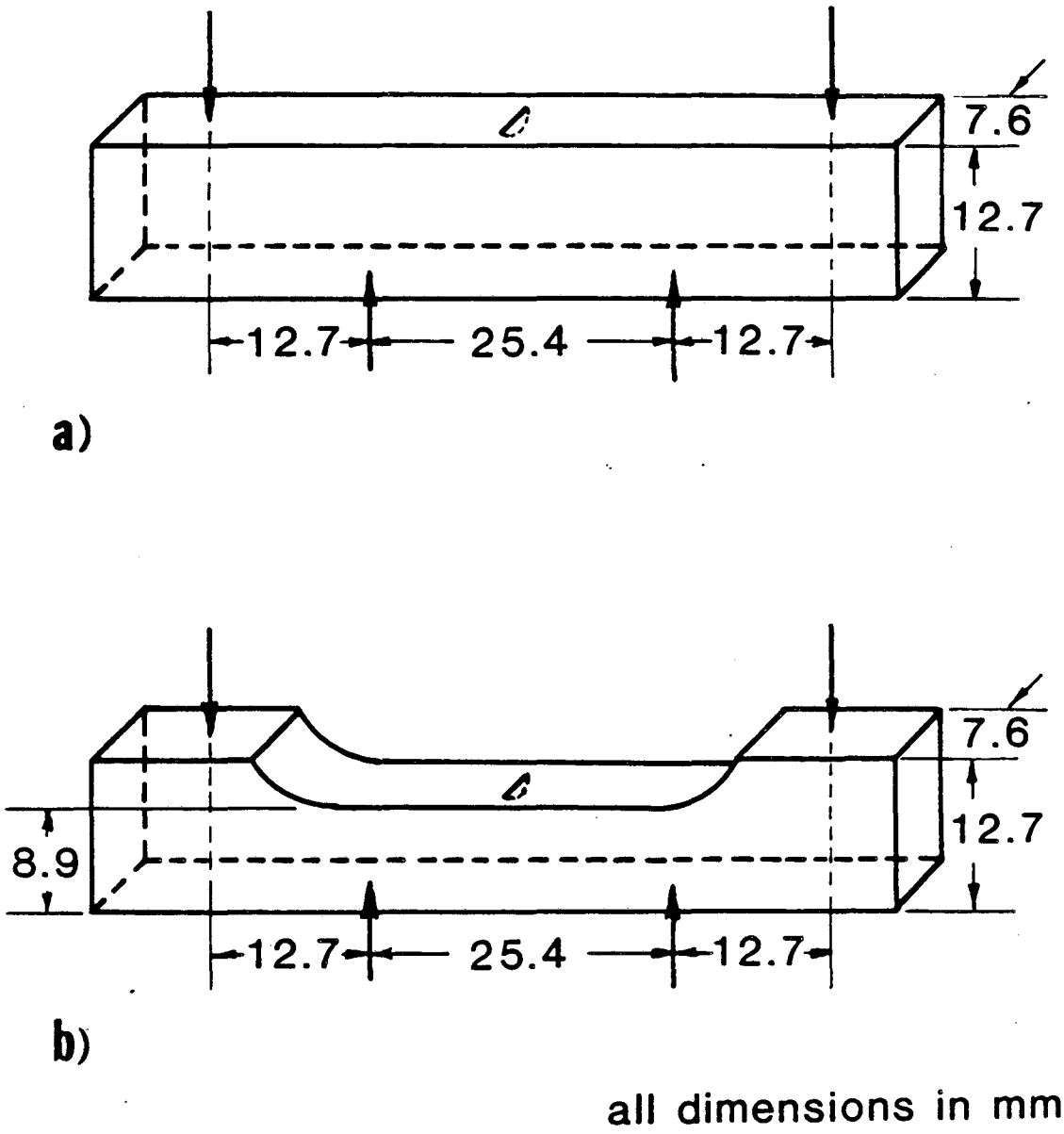

Fig. 1: a) Smooth and b) waisted geometries of four-point bend specimens used to measure small crack growth rates.

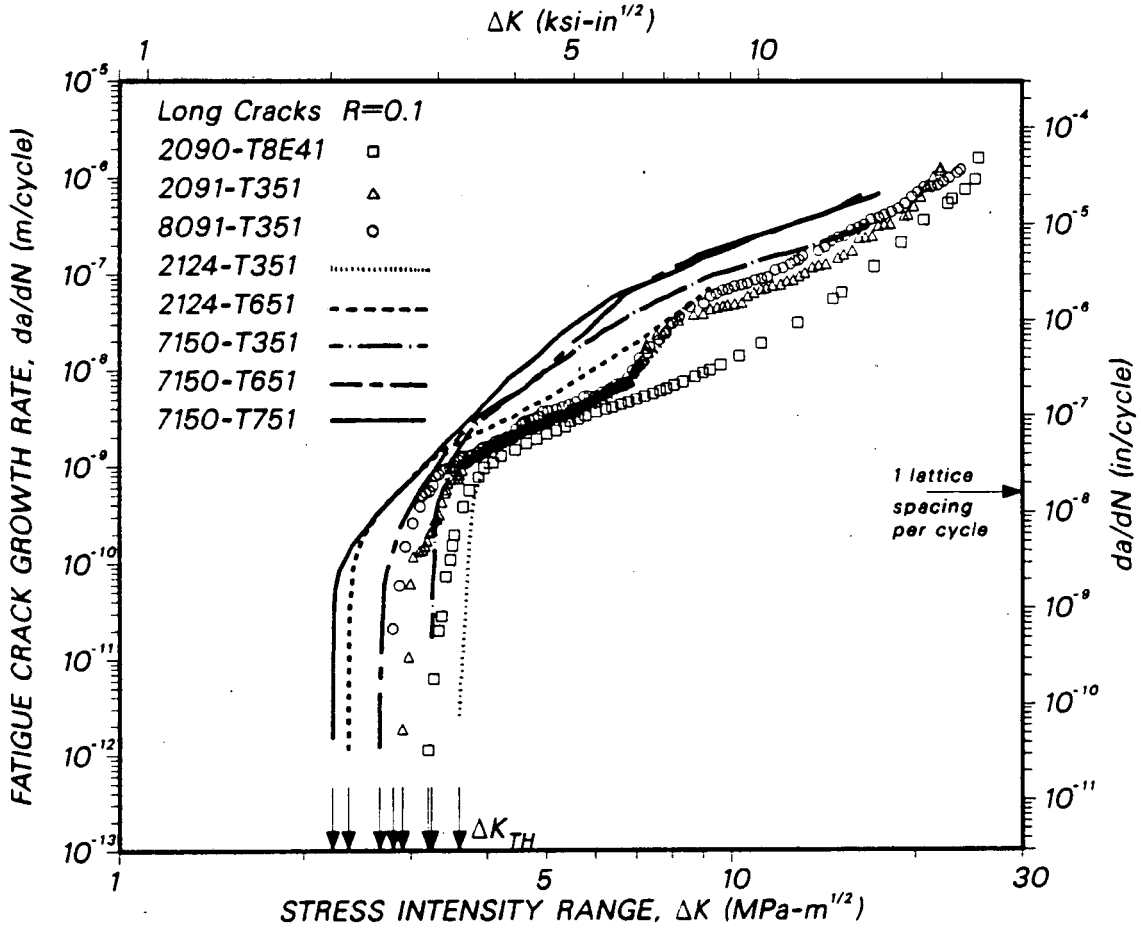

Fig. 2: Variation in fatigue crack growth behavior (at R = 0.1) with nominal stress intensity range ΔK, for long (≳ 10 mm) cracks in commercial high-strength aluminum alloys. Note how lithium containing alloys, 2090, 2091 and 8091, tend to display the lowest growth rates.

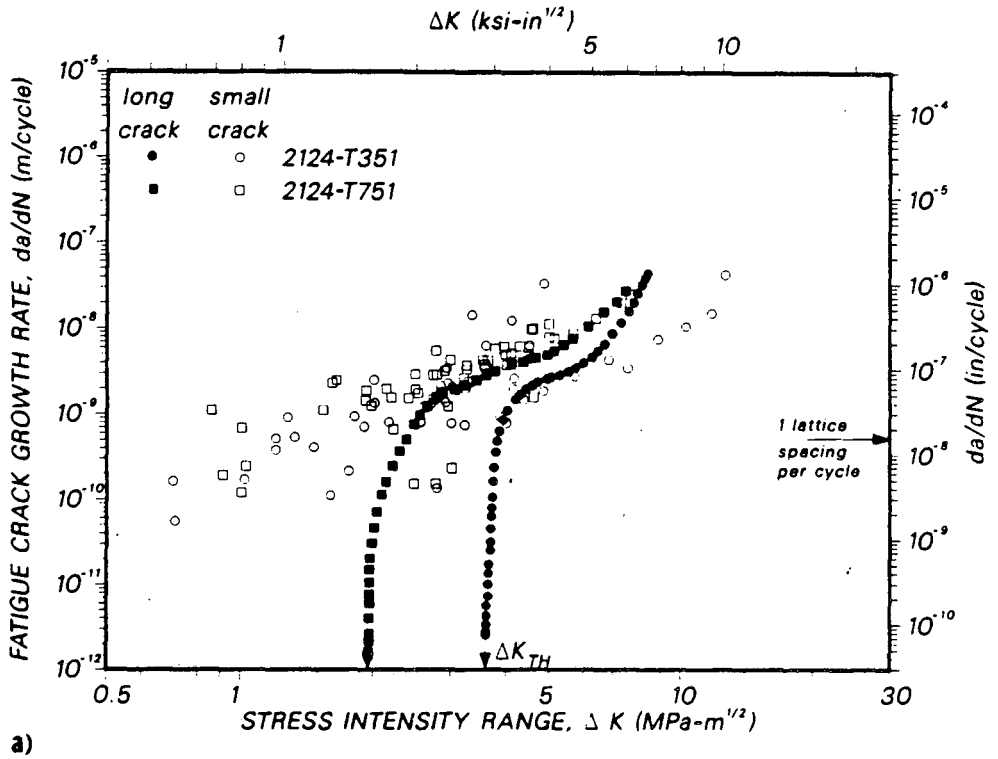

a)

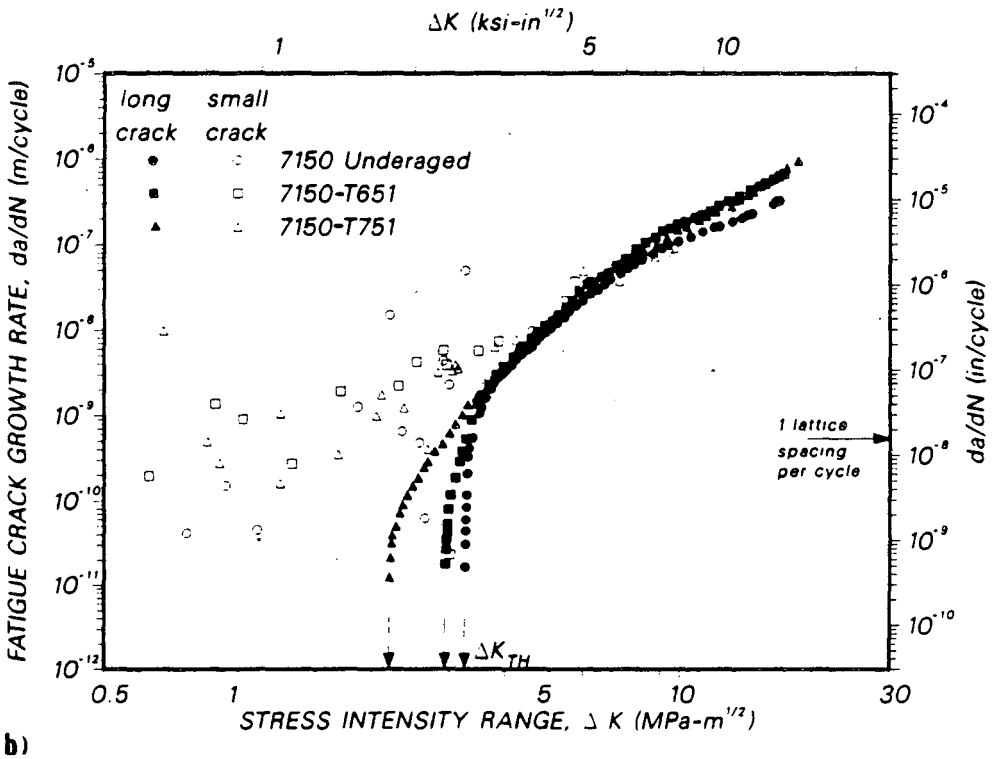

b)

Fig. 3: Comparison of long ($\gtrsim$10 mm) and small (1-1000 μm) fatigue crack growth rate behavior (at R = 0.1) in a) underaged (T351) and overaged 2124 alloy, and b) underaged, peak aged (T651) and overaged (T751) 7150 alloy.

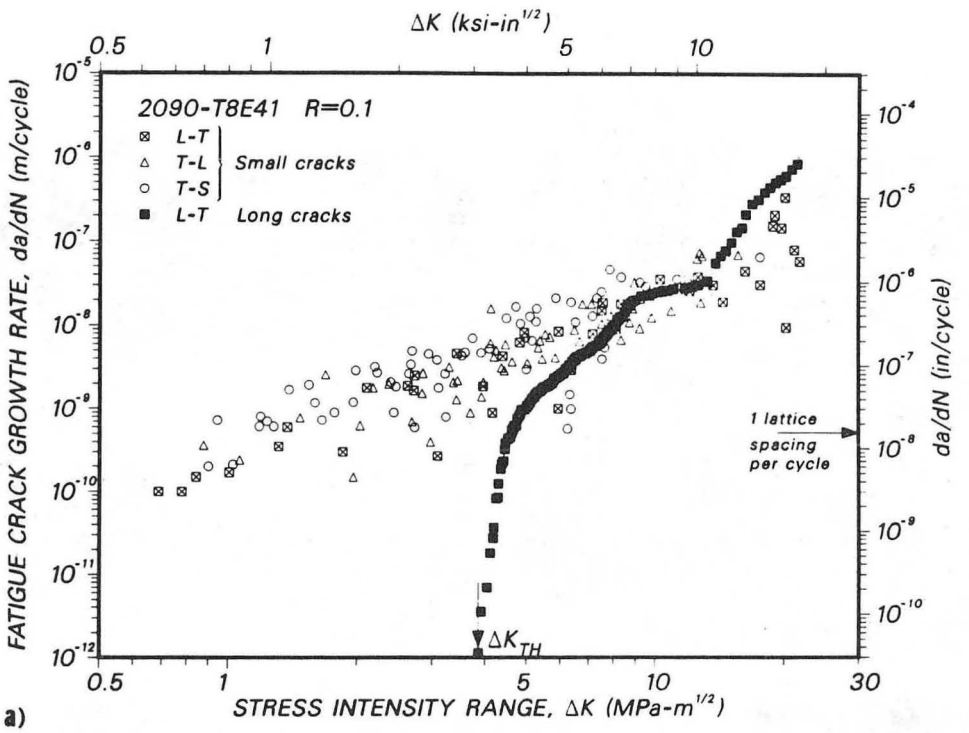

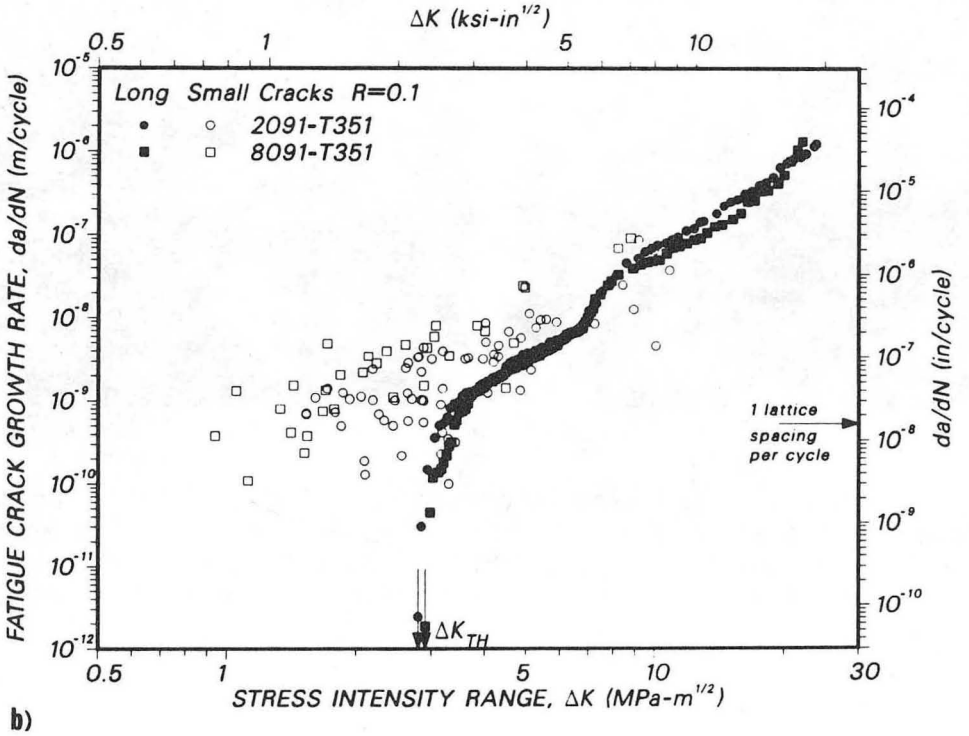

Fig. 4: Comparison of long ($\gtrsim$10 mm) and small (1-1000 μm) fatigue crack growth rate behavior (at R = 0.1) in aluminum-lithium alloys, showing results for the L-T, T-L and T-S orientations in 2090-T8E41, and b) the L-T orientation in 2091-T351 and 8091-T351.

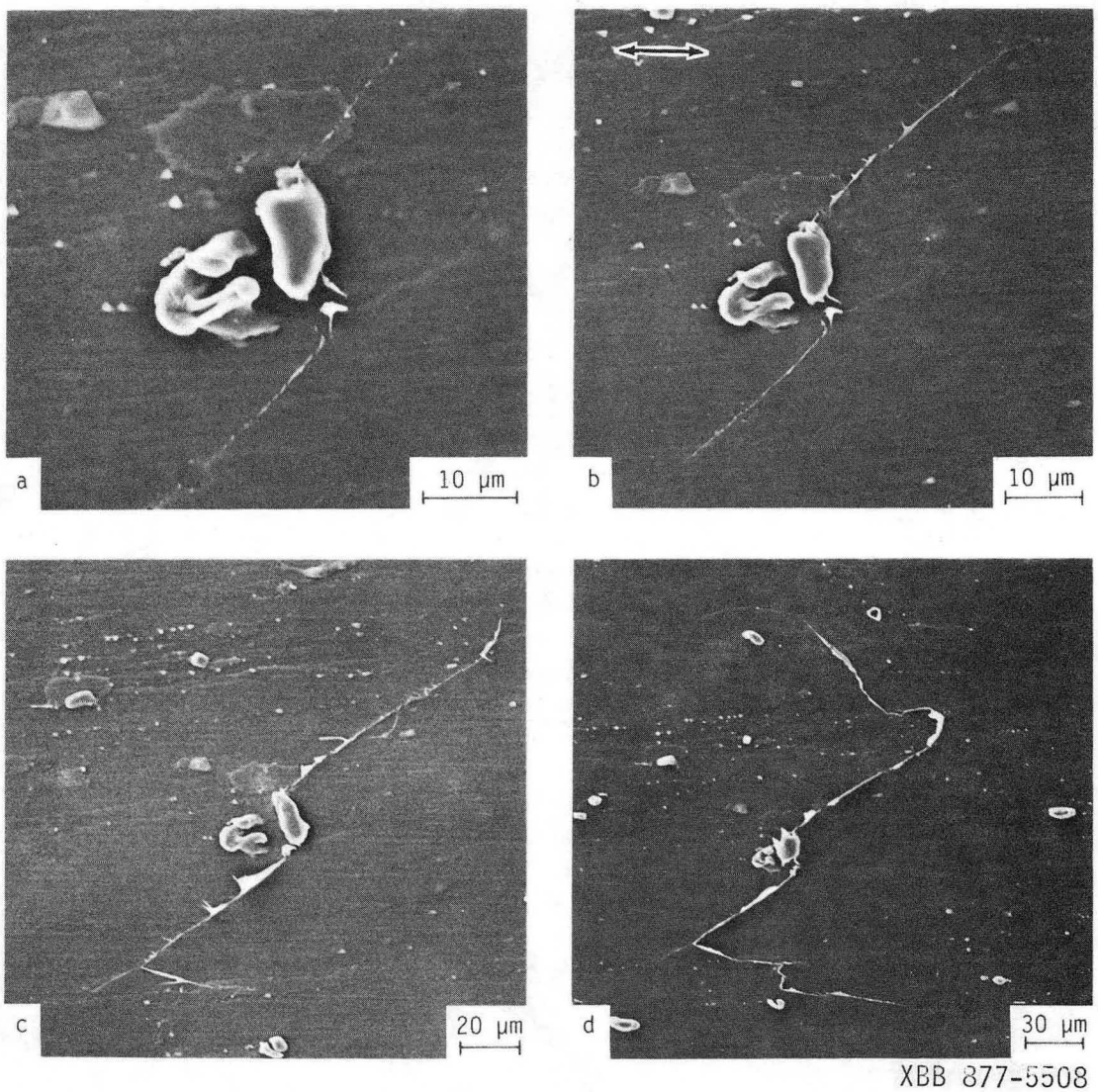

Fig. 5: Scanning electron micrographs of gold coated acetate replicas of initiation and deflected crack growth of small cracks in 2091-T351, measured at a) 70,000, b) 80,000, c) 90,000, and d) 100,000 cycles following crack initiation. Arrow represents the direction of applied stresses.

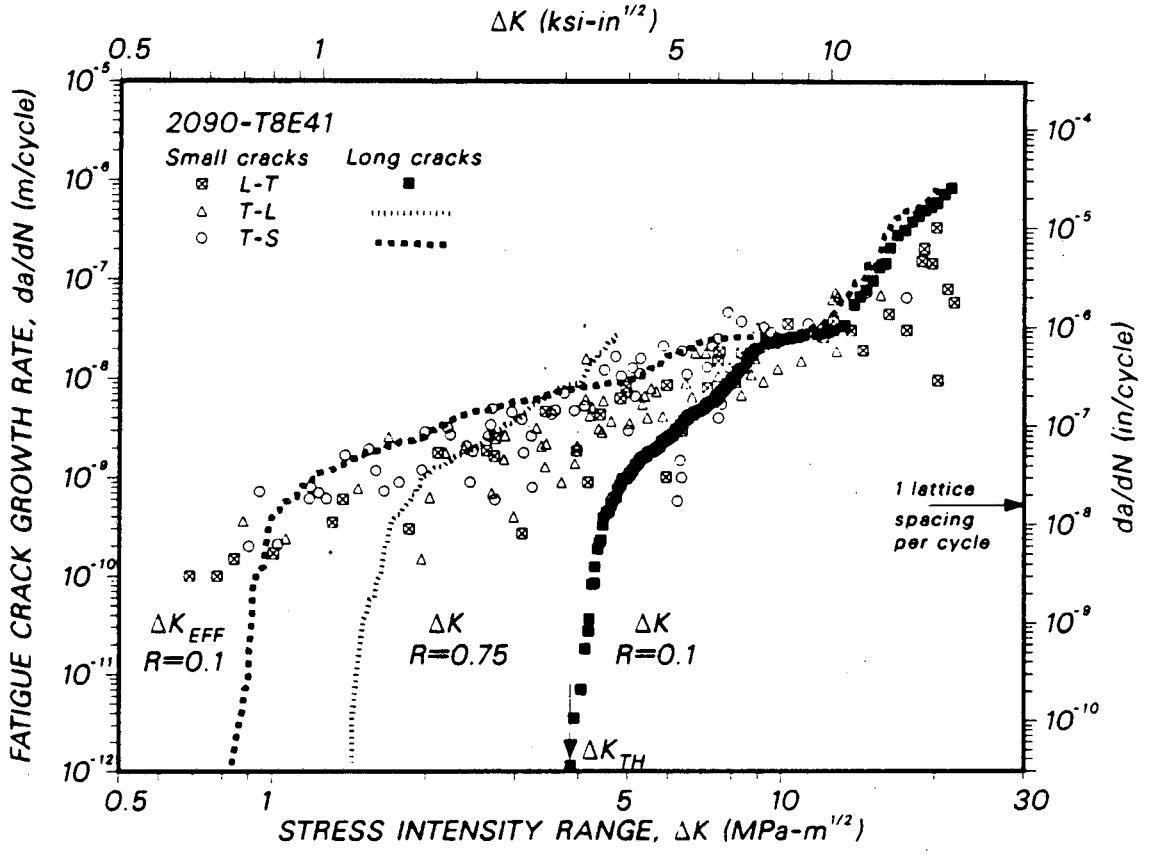

Fig. 6: Long (≳10 mm) and small (1-1000 μm) fatigue crack growth rate behavior (at R = 0.1) in aluminum-lithium alloy 2090-T8E41 as a function of ΔK, showing comparison with i) long crack data characterized in terms of ΔK_{eff}, and ii) long crack data monitored at high load ratios (R = 0.75).

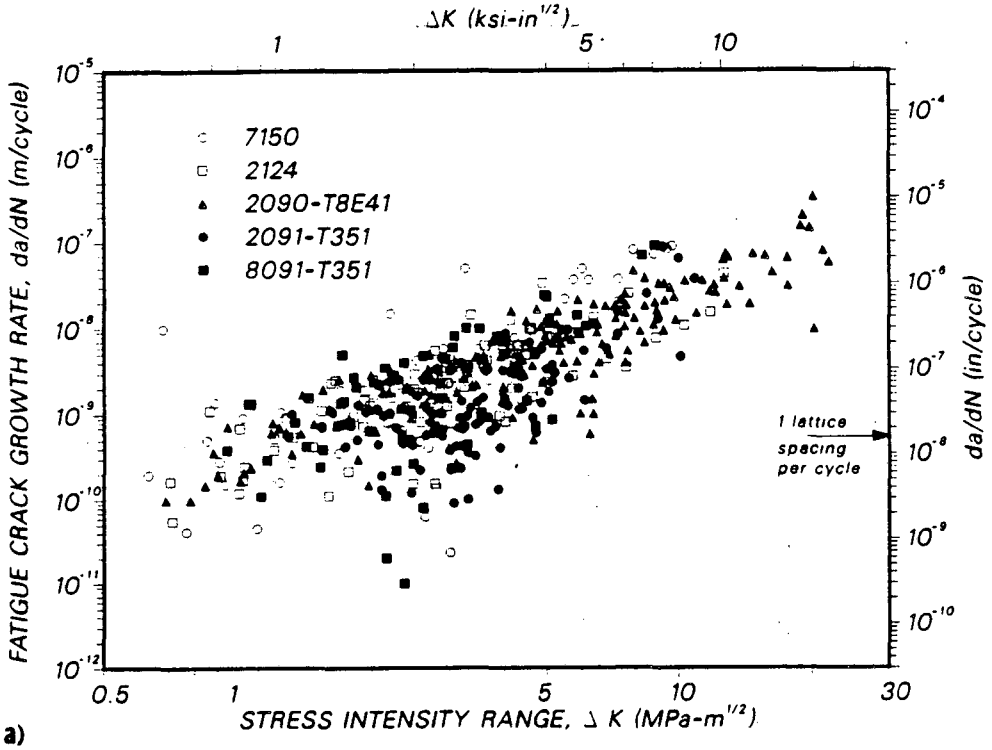

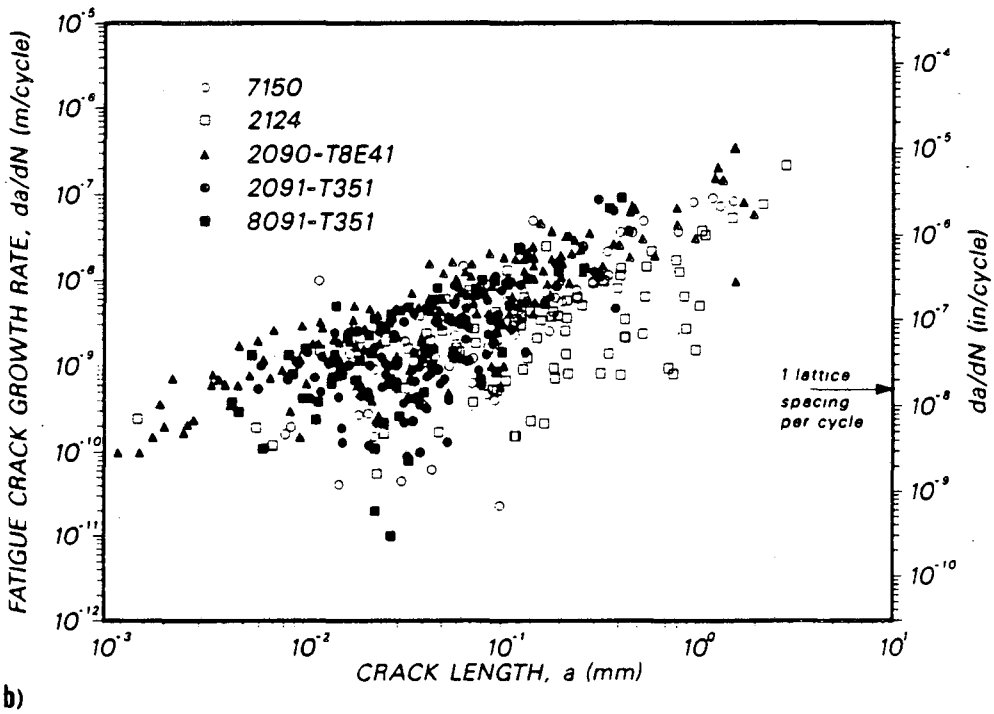

Fig. 7: Variation of the fatigue crack propagation rates of small (1-1000 μm) surface cracks in commercial aluminum alloys as a function of a) nominal stress intensity range (ΔK) and b) crack length (a). Data are compared for aluminum-lithium alloys 2090-T8E41, 2091-T351 and 8091-T351, and traditional high-strength alloys 2124 and 7150 in various aging conditions.

LAWRENCE BERKELEY LABORATORY
TECHNICAL INFORMATION DEPARTMENT
UNIVERSITY OF CALIFORNIA
BERKELEY, CALIFORNIA 94720